Available online at www.sciencedirect.com
SCIENCE DIRECT®
Polymer 44 (2003) 3229–3234
polymer
www.elsevier.com/locate/polymer

Staining of poly(ethylene terephthalate) by ruthenium tetroxide

H.G. Haubruge*, A.M. Jonas, R. Legras

Université catholique de Louvain, Laboratoire de Physique et de Chimie des Hauts Polymères, Croix du Sud 1, B-1348 Louvain-la-Neuve, Belgium

Received 21 August 2002; received in revised form 24 February 2003; accepted 18 March 2003

Abstract

The staining of poly(ethylene terephthalate) (PET) by ruthenium tetroxide (RuO_4) is used to obtain a contrast at the crystalline lamellar scale in transmission electron microscopy. This paper demonstrates the efficiency of this technique conducted in vapor phase on ultracut bulk samples. Advantages of this method against other contrast enhancing techniques and the parameters of staining are discussed. The depth of attack is measured and is shown to be limited by a crosslinking process. The chemical mechanisms are investigated by grazing infrared spectroscopy and involve the oxidation of the aliphatic moeities of PET.
© 2003 Elsevier Science Ltd. All rights reserved.

Keywords: Lamellar resolution; Poly(ethylene terephthalate); RuO_4 staining

1. Introduction

Since its introduction from the fields of cellular biology and histology [1], the ruthenium tetroxide (RuO_4) staining technique has been widely used to obtain an improved image contrast in the transmission electron microscopy (TEM) of a number of polymers. Apart from its use in the study of polymer blends [2–9], this method was in some cases also successful in producing a contrast at a lamellar resolution, i.e. between the crystalline polymer lamellae and the amorphous regions, for semi-cristalline homopolymers [8–18] or block copolymers [15,19,20].

Other adequate staining reagents for that purpose include a.o. chlorosulphonic acid ($ClSO_3H$) and osmium tetroxide (OsO_4). In the first case, a chlorosulphonic acid attack followed by an uranyl acetate staining proved to be efficient for polyethylene, but was of limited applicability for other polymers [14,21]. On the other hand, osmium tetroxide long remained the reagent of choice for unsaturated polymers [22] but its lack of reactivity towards aromatic and saturated aliphatic polymers, and the two-step staining process that it often required, led to the adoption of the stronger oxidizer RuO_4.

First introduced by Trent [10] who studied its interaction in a number of polymer systems, its use was later refined by Montezinos [11] who proposed its in situ production by the means of a reaction between ruthenium trichloride ($RuCl_3$) and aqueous sodium hypochlorite (NaClO). It was first applied to polyethylene and polypropylene but its use was quickly extended to a large variety of polymers.

Regarding polyesters, while staining of poly(butylene terephthalate) (PBT) [15] or polycarbonate (PC) [3,6] proved easy enough, poly(ethylene terephthalate) (PET) staining is reputedly very difficult. As a matter of fact, only two mentions of a lamellar contrast obtained by TEM on stained samples are found in the litterature for pure PET. The first uses OsO_4 as reagent [23] but this result was later criticized as being non-reproducible [24]. Other attempts of OsO_4 staining were based on a two-step process involving prior attack by a double-bond containing reagent. They did not, however, succeed in providing lamellar-scale contrast. The second claim of lamellar contrast obtention for pure PET, using a ruthenium-based technique similar to the one described here, was made more recently [25]. This followed a noticeable observation of isolated lamellar stacks of PET in a poly(ether imide) (PEI) blend [9].

Other techniques have also contributed to the study of the lamellar microstructure of PET, but each of these techniques has its drawbacks and limitations. PET single crystals were isolated after hydrolysis [26], but scanning electron microscopy (SEM) on samples etched by aminolysis [27] or plasma only allowed, by removal of the less ordered zones, the observation of gross superstructures.

* Corresponding author. Tel.: +32-10473391; fax: +32-10451593.
E-mail address: haubruge@poly.ucl.ac.be (H. H.G.).

0032-3861/03/$ - see front matter © 2003 Elsevier Science Ltd. All rights reserved.
doi:10.1016/S0032-3861(03)00255-6

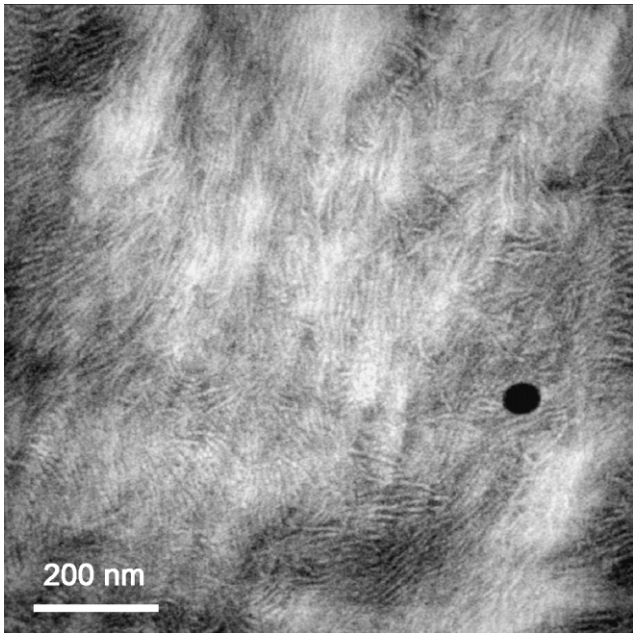

Fig. 1. TEM micrograph of RuO_4-stained PET.

Micrographs of carbon replicas [28] revealed a lamellar structure but this technique does not allow quantitative evaluation of the morphology.

Recent results obtained by atomic force microscopy (AFM) [29] revealed the lamellar structure at the surface of films and even allowed a real-time study of the crystallization process. Despite this interesting result, the direct observation of the lamellar morphology of PET by TEM still offers much interest. Although it does not support real-time crystallization study, the technique is not limited to thin films but can also be applied to sections of bulk samples. This therefore yields observations free of confinement and free surface effects characteristic of thin films, so far a major drawback of most AFM-based observations.

In this context, this paper proposes a simple and efficient staining technique to reach lamellar-scale contrast for PET. The described method is based on the exposition of ultracut polymer samples or thin films to the vapor of RuO_4, produced in situ from the reaction of $RuCl_3$ and aqueous NaClO. The parameters, mechanisms and efficiency of this system are discussed.

2. Experimental

PET, grade E47 ($M_n \simeq 20000$), was obtained from Imperial Chemical Industries. Small pellets (20 mg) were isothermally crystallized from the melt at 230 °C for 1 h under a nitrogen flow in a Perkin Elmer DSC7, then quenched at room temperature. These samples were faced using a glass knife then cut at room temperature on a Reichert ultracut equipped with a diamond knife. Ultrathin sections (50–100 nm thick) were deposited on 400-mesh TEM copper grids.

Ruthenium tetroxide used for staining was produced in situ by mixing 0.1 g ruthenium trichloride hydrate (Acros) with 5 ml of 13% active chlorine aqueous sodium hypochlorite (Acros). The polymer sections were exposed, at room temperature, to vapors of this freshly made solution for times ranging from 5 min to 1 h. Stained and unstained samples were observed in a Philips EM 301 transmission electron microscope operating at 80 kV. For staining experiments performed below or above room temperature, the closed vessel containing sample and stain was simply placed in a freezer or oven, respectively.

PET thin films were obtained by spincoating a 50 g/l solution of PET in hexafluoroisopropanol (HFIP, Acros) on floated glass, silicon and gold-coated silicon. Their thickness was characterized with a Jobin Yvon ellipsometer and is about 200 nm (the refractive index of PET was first estimated from a set of measurements performed on PET films spincoated from solutions with varying concentrations). 20 μm-thick films were produced by solvent-casting the same solution on floated glass. Amorphous 100 μm-thick films were obtained by melt-pressing PET between Kapton polyimide sheets using an aluminum intercalate, then quenching it in cold water. These films were stained using the above-described method.

FTIR transmission spectra were recorded on a Perkin Elmer model 1760-X spectrophotometer (4 cm^{-1} resolution). IRAS (Infrared Reflection Absorption Spectroscopy) spectra were obtained on a Bruker Equinox 55 FTIR (4 cm^{-1} resolution) with a grazing beam accessory (non-polarized light at incident angle of 80°). The spectra were baseline corrected and absorbance-normalized on the 732 cm^{-1} β–C=O phenyl peak. Peaks were assigned according to Daniels and Kitson [30] and more recent results [31].

EDS (Energy Dispersion Spectroscopy) elemental microanalysis and cartography was conducted on a high resolution FEG Digital Scanning Microscope 982 Gemini from Leo operating at 25 keV, equipped with a Phoenix EDAX detector.

Steric exclusion chromatography (SEC) analysis was performed with a 98:2 vol. mixture of chloroform and HFIP as solvent. Two Waters HR5E Styragel columns were used in series with a 0.8 ml/min flow rate. Detection was made by a Waters 484 UV detector at 254 nm. A universal calibration curve was obtained from polystyrene (PS) standards using the Mark-Houwink coefficients for PS and PET published by Weisskopf [32].

3. Results

3.1. Staining parameters

Fig. 1 displays clearly resolved lamellae in a bulk PET

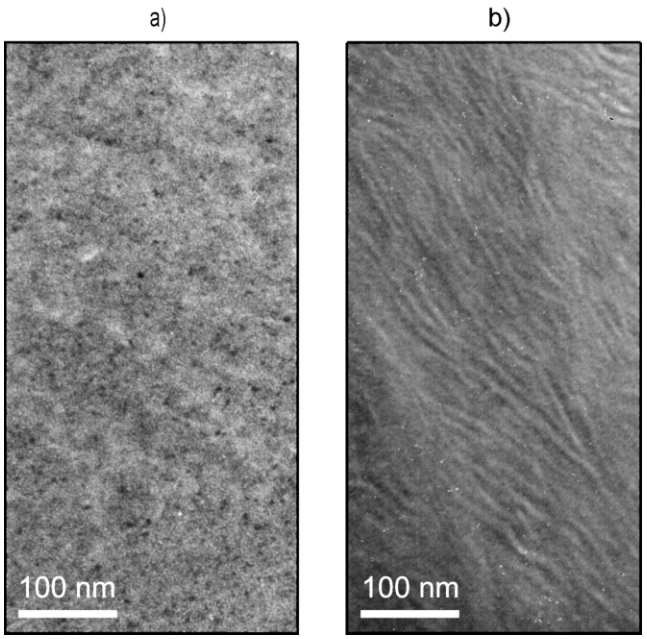

Fig. 2. TEM micrographs of PET stained at (a) 80 °C for 15 min and (b) − 15 °C for 2 h.

sample stained for 15 min at room temperature according to the conditions described in Section 2. This result alone allows interesting studies about the crystalline morphology of PET that will be the subject of a following paper [33]. This section will, however, concentrate on the varying parameters that account for this empirical success.

Qualitative analysis based on visual control of the image contrast shows that the duration of staining has an obvious cumulative effect. In addition, temperature was also found to be an important kinetic factor since conducting the staining procedure at 80 °C caused a fast sample 'burning',

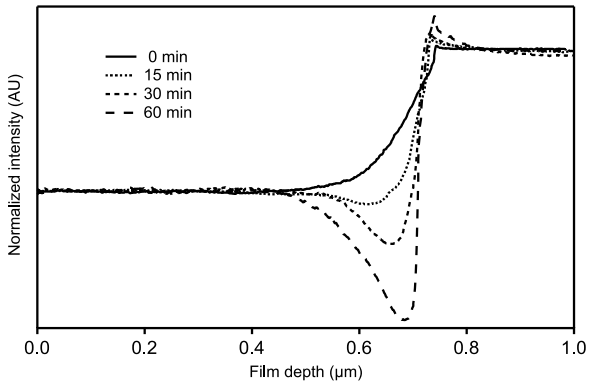

Fig. 4. One-dimensional average of staining profiles: staining time of (a) 0 min, (b) 15 min, (c) 30 min and (d) 60 min.

characterized by the destruction of polymer crystals and the appearance of numerous small RuO_2 aggregates. On the opposite, a temperature as low as − 15 °C required staining times of about 2 h to obtain a proper contrast, as is shown in Fig. 2. The regulation of the staining atmosphere also appeared to play a major part. A closed system procedure favors fast saturation of the atmosphere. A suitable displacement of the equilibrium of RuO_4 vapor formation is, on the other hand, also favorable. This was obtained by placing an easily oxidized material, such as commercial polypropylene, in a glass staining cell or by simply using a polypropylene container, acting as sinks for the RuO_4 vapor. Poorer results were obtained for experimental setups not containing a RuO_4 sink.

3.2. Depth of attack

The knowledge of the depth reached by RuO_4 staining is important in order to evaluate the significance of the morphology observed on ultracut samples. Amorphous

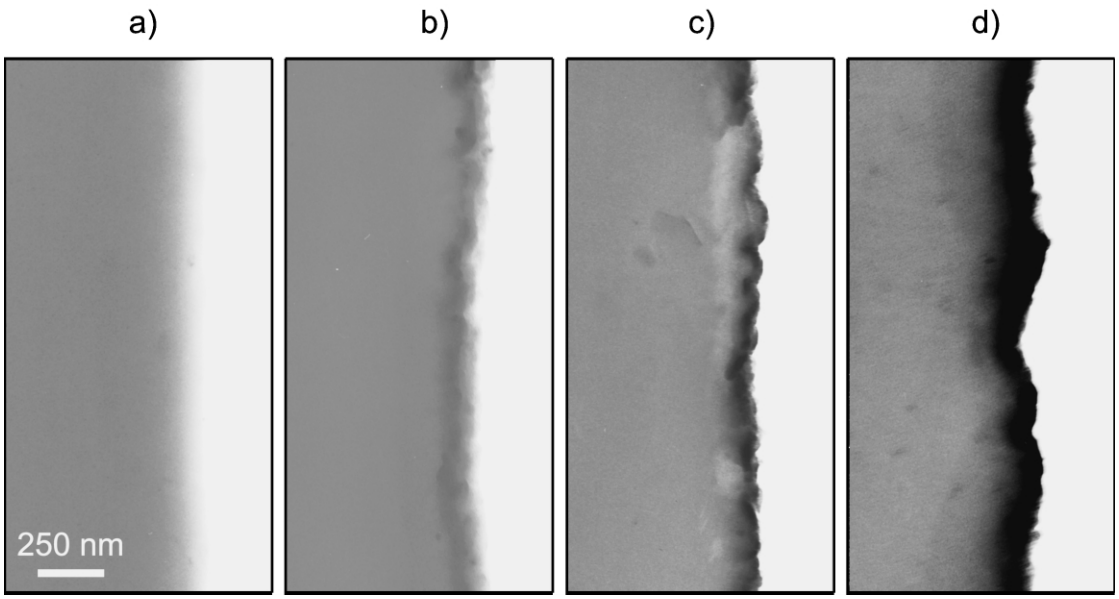

Fig. 3. Staining profiles of a 100 μm-thick PET film observed by TEM on a cross-section: staining time of (a) 0 min, (b) 15 min, (c) 30 min and (d) 60 min.

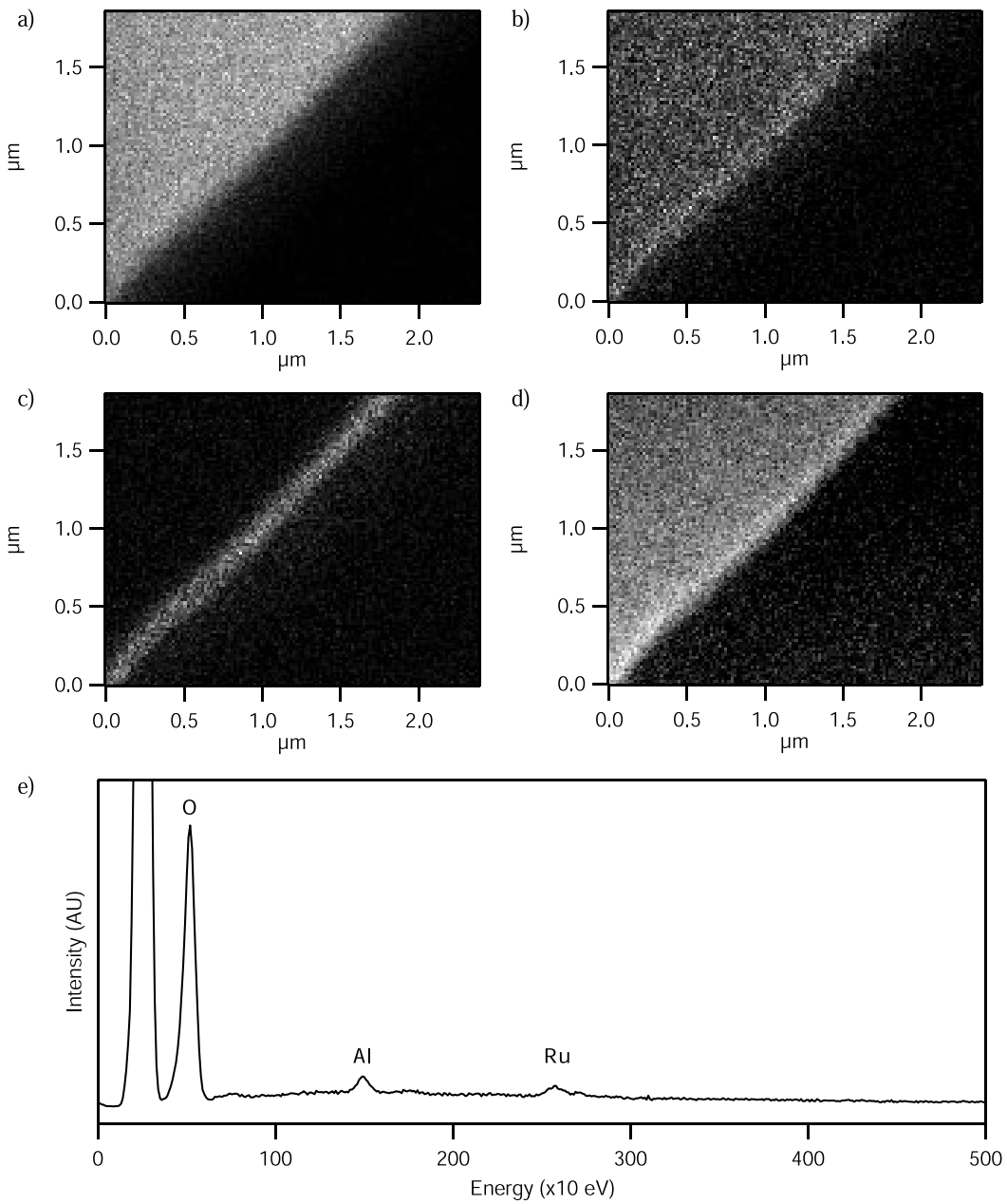

Fig. 5. Staining profile of a 100 µm-thick PET film, RuO_4-stained for 30 min, observed by EDS: (a) carbon, (b) oxygen, (c) ruthenium, (d) secondary electrons image and (e) EDS spectrum from the stained part of the sample.

thick films (100 µm) of PET were thus stained for varying times and transversally cut to determine their staining profile.

Direct TEM observation of these samples reveals a dark, very contrasted and somewhat irregular surface layer corresponding to the stained zone, as can be seen in Fig. 3. Its roughness might be attributed to cut-induced distorsion, since in some places a separation of the skin from the bulk was even observed. This also indicates the strong cohesion of the stained layer. Its thickness is evaluated as 180 nm and does not vary much with staining time. On the contrary, the intensity of staining, semi-quantitatively determined by the normalized contrast of TEM micrographs of the surface layer, does increase with staining time, as is shown in Fig. 4.

3.3. Chemical reactions

A SEM-EDS analysis confirms the presence of ruthenium in the contrasted layer, as well as a parallel increase in oxygen concentration (see Fig. 5). Chlorine is not detected within the sensitivity of the instrument, while aluminum traces come from the sample holder. The measured thickness of the stained zone is about 170 nm, which

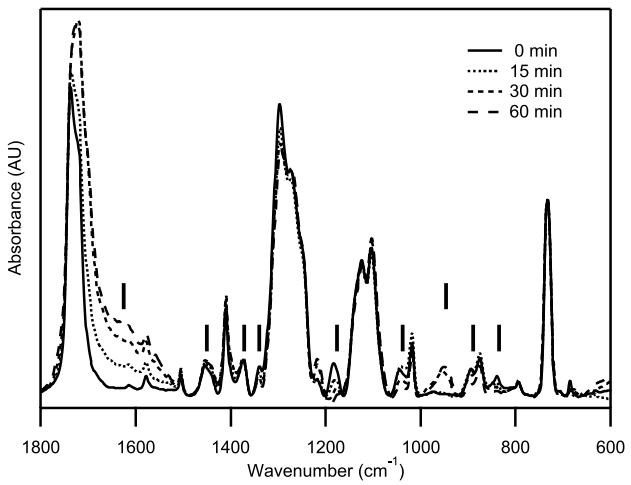

Fig. 6. Infrared spectra (IRAS) of PET thin films stained for increasing times. Decreasing CH_2 peaks and increasing bands at 1640 and 950 cm^{-1} are highlighted.

correlates well with the length obtained from TEM. The chemical mechanisms underlying the staining effect were further probed using infrared spectroscopy in grazing incidence reflection mode (Fig. 6).

Being normalized on a phenyl peak (see Section 2), the spectra obviously contain few variations for other phenyl peaks. A noticeable exception to this is the decreasing band at 1183 cm^{-1}, but this peak has sometimes been attributed to CH_2 twisting [34] too. As regards CH_2 peaks, most of them decrease (1341, 1042, 895 and 840 cm^{-1}). However, other CH_2 peaks stay almost unchanged (1373 cm^{-1}) or even slightly increase (1450 cm^{-1}). But so is the phenyl peak at 1410 cm^{-1}, which lead us to conclude to the insignificance of these local discrepancies, maybe due to the appearance of a broad peak around 1430 cm^{-1}. One thus notices a global decrease of CH_2 groups.

While the C–O–C triplet (1266 cm^{-1}) stays almost constant, the C=O stretching band (1730 cm^{-1}) both increases and shifts. An important unknown peak also appears at 950 cm^{-1}. Finally, wavenumbers above

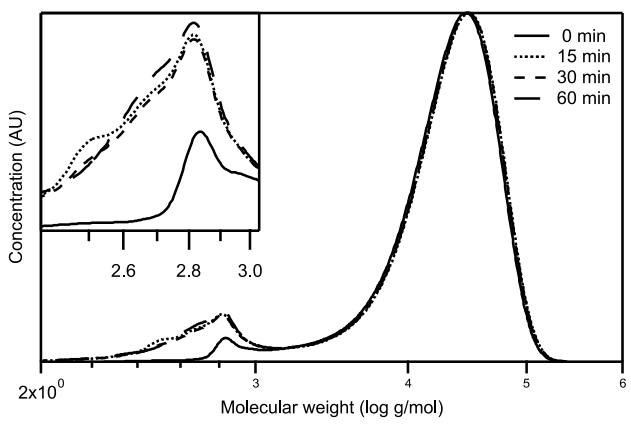

Fig. 7. Steric exclusion chromatograms with varying staining times.

1800 cm^{-1} are dominated by intense broad peaks around 3400 and 2740 cm^{-1}, at least partly due to the buildup of water, which is also noticed at 1640 cm^{-1}.

Another information on the chemical mechanism is provided by the observed insolubility of the stained surface layer in HFIP. The whole thin film is actually seen floating off, indicating a very cohesive nature. This directly hints to a crosslinking mechanism. SEC performed on the soluble fraction of the film shows an almost constant weight-averaged molar weight at about 30,000 g/mol (see Fig. 7), concurrently with the appearance of compounds with molar weights smaller than PET cyclic oligomers.

4. Discussion and conclusion

Staining by ruthenium tetroxide is admittedly due to the precipitation of fine ruthenium dioxide particles, resulting from the local oxidation of the amorphous phase of the polymer. The presence of these localized electron-rich particles creates contrast in TEM imaging. A nodular background on the nanometer scale is indeed visible on TEM micrographs of PET, possibly due to deposited RuO_2 nanocrystals [35]. Obviously, a deposition of RuO_2 crystals on the surface only does not occur since the modified depth was determined to be about 180 nm. Large-scale surface RuO_2 crystals are more probably linked to long attack durations or high temperatures leading to the overoxidation of the sample.

As regards the chemical mechanisms of staining, infrared analysis mainly suggests an oxidation of the aliphatic moeities of PET only, with the rise of new C=O and few unknown peaks. The role of chlorine is unknown, but a catalytic action was suggested [8]. Concurrently, cross-linking occurs, resulting a.o. in a much higher mechanical cohesion and a well-known stabilizing effect against electron beam damage. At the same time, the marked ruthenium concentration front confirms that the crosslinked and stained layer is an obstacle to further diffusion of the staining agent [16].

Historically, Trent [10] considered that polyolefins were stainable only thanks to the presence of unsaturated groups, while PET could be stained through its hydroxyl chain-ends. Present results, as well as those obtained for PE and PP [12], rather highlight an oxidation mechanism of CH_2 groups. In the case of PET, aromatic rings are indeed protected against oxidation by their electron-withdrawing neighbouring groups. This may cast a new light on previous results: PBT, subject to the same protection, is probably more easily stained than PET because of both its longer aliphatic chain and its lower glass transition temperature, thus higher diffusion rate of RuO_4. This might also explain why bisphenol-A polycarbonate (PC), with its electron-donating CH_3 near the phenyl, is preferentially stained in PC/PBT blends, as was already pointed out [4,6]. Staining by ruthenium tetroxide is nevertheless a complex solid-state

reaction and one should be careful before applying these conclusions to other polymer blends.

In this paper, we were able to determine a set of staining conditions for poly(ethylene terephthalate) allowing observation of the crystalline morphology at the lamellar scale. This method is useful for thin films but also for sections from the bulk, from pure PET or from blends. Such a successful staining, which results from a delicate equilibrium between reactivity and diffusion, will be exploited in a coming paper to study in detail the semi-crystalline morphology of PET [33].

Acknowledgements

The authors would like to thank Mark Koetse for his expertise in the IRAS technique and Pascale Lipnik for her help with the ultramicrotomy and staining methods. They are also indebted to Pr. Jacques Devaux for many fruitful discussions. They gratefully acknolewdge financial support of this work by the Fonds National de la Recherche Scientifique.

References

[1] Gaylarde P, Sarkany I. Science 1968;161:3846.
[2] Trent JS, Scheinbeim JI, Couchman PR. J Polym Sci Polym Lett Ed 1981;19:315.
[3] Hobbs SY, Dekkers MEJ, Watkins VH. J Mater Sci 1988;23:1219.
[4] Delimoy D, Bailly C, Devaux J, Legras R. Polym Engng Sci 1988; 28(2):104.
[5] Tervoort-Engelen Y, Van Gisbergen J. Polym Commun 1991;32:261.
[6] Delimoy D, Goffaux B, Devaux J, Legras R. Polymer 1995;36(17): 3255.
[7] Brown GM, Butler JH. Polymer 1997;38:3936.
[8] Ivanov DA, Lipnik PDM, Jonas AM. J Polym Sci Part B: Polym Phys 1997;35:2565.
[9] Ivanov DA, Pop T, Yoon DY, Jonas AM. Proc ACS: Div Polym Mater Sci Engng (ACS Fall meeting, August, New Orleans, USA) 1999;81: 335.
[10] Trent JS, Scheinbeim JI, Couchman PR. Macromolecules 1983;16: 589.
[11] Montezinos D, Wells BG, Burns JL. J Polym Sci: Polym Lett Ed 1985; 23:421.
[12] Sano H, Usami T, Nakagawa H. Polymer 1986;27:1497.
[13] Cao T, Chen S, Jin Y. Polym Commun 1988;29:66.
[14] Kunz M, Heinrich UR, Möller M, Cantow HJ. Prog Coll Polym Sci 1988;77:238.
[15] Janik H, Walch E, Gaymans RJ. Polymer 1992;33(16):3522.
[16] Huong DM, Dreschler M, Cantow HJ, Möller M. Macromolecules 1993;26:864.
[17] Li JX, Ness JN, Cheung WL. J Appl Polym Sci 1996;59:1733.
[18] Li JX, Cheung WL. J Appl Polym Sci 1999;72:1529.
[19] Khandpur AK, Macosko CW, Bates FS. J Polym Sci, Part B: Polym Phys 1995;33:247.
[20] Hong S, Bushelman AA, MacKnight WJ, Gido SP, Lohse DJ, Fetters LJ. Polymer 2001;42:5909.
[21] Kanig G. Prog Coll Polym Sci 1975;57:176.
[22] Kato KJ. Electron Microsc 1965;14:220.
[23] Watkins NC, Hansen D. Text Res J 1968;32:388.
[24] Wegner G, Zhu LL, Lieser G. Makromol Chem 1981;182:231.
[25] Xia Z, Sue HJ, Wang Z, Avila-Orta CA, Hsiao BS. J Macromol Sci Phys 2001;B40(5):625.
[26] Miyagi A, Wunderlich BJ. Polym Sci, Part A2: Polym Phys 1972;10: 2073.
[27] Chu CM, Wilkes GL. J Macromol Sci Phys 1974;B10(4):551.
[28] Groeninckx G, Berghmans H, Smets G. J Polym Sci: Polym Phys 1976;14:591.
[29] Ivanov DA, Amalou Z, Magonov SN. Macromolecules 2001;34(26): 8944.
[30] Daniels WW, Kitson RE. J Polym Sci 1958;23:161.
[31] Cole KC, Ajji A, Pellerin E. Macromolecules 2002;35(3):770.
[32] Weisskopf KJ. Polym Sci, Part A: Polym Chem 1988;26:1919.
[33] Haubruge HG, Jonas AM, Legras R. 2003. Manuscript in preparation.
[34] Miyake AJ. Polym Sci 1959;38:497.
[35] Chou TM, Prayoonthong P, Aitouchen A, Libera M. Polymer 2002; 43:2085.